

1 **Modeling the growth and sporulation dynamics of the macroalga *Ulva* in mixed-age**
2 **populations in cultivation and the formation of green tides**

3 Uri Obolski^{1,2,*}, Thomas Wichard³, Alvaro Israel⁴, Alexander Golberg¹, Alexander Liberzon^{5,*}

4 ¹ Porter School of the Environment and Earth Sciences, Tel Aviv University, Tel Aviv, Israel

5 ² School of Public Health, Tel Aviv University, Tel Aviv, Israel

6 ³ Institute for Inorganic and Analytical Chemistry, Friedrich Schiller University Jena, Jena, Germany

7 ⁴ Israel Oceanographic & Limnological Research Ltd. (PBC), Tel Shikmona, Haifa, Israel

8 ⁵ School of Mechanical Engineering, Tel Aviv University, Tel Aviv Israel.

9 ***Correspondence should be addressed to:**

10 Uri Obolski: uriobols@tauex.tau.ac.il

11 Alexander Liberzon: alexlib@tauex.tau.ac.il

12 **Abstract**

13 *Ulva* is a widespread green algal genus with important ecological roles and promising potential as a
14 seagiculture crop. One of the major challenges when cultivating *Ulva* is sudden biomass disappearance,
15 likely caused by uncontrolled and unpredicted massive sporulation. However, the dynamics of this process
16 are still poorly understood. In this study, we propose a mathematical model describing the biomass
17 accumulation and degradation of *Ulva*, considering the potential impact of sporulation inhibitors. We
18 developed a differential equation model describing the time evolution of *Ulva* biomass. Our model
19 simulates biomass in compartments of different *Ulva* ‘age’ classes, with varying growth and sporulation
20 rates. Coupled with these classes is a differential equation describing the presence of a sporulation inhibitor,
21 produced and secreted by the algae. Our model mimics observed *Ulva* dynamics. We present *Ulva*’s
22 biomass accumulation under different initial algae population, age distributions and sporulation rates.
23 Furthermore, we simulate water replacement, effectively depleting the sporulation inhibitor, and examine
24 its effects on *Ulva*’s biomass accumulation. The model developed in this work is the first step towards
25 understanding the dynamics of *Ulva* growth and degradation. Future work refining and expanding our
26 results should prove beneficial to the ecological research and industrial growth of *Ulva*.

27

28 **Keywords:** *Ulva*, sporulation, sporulation inhibitor, modeling, green tides, gametogenesis, aging,
29 aquaculture management.

30

31 1. Introduction

32 The genus *Ulva* (Ulvales, Chlorophyta) comprises a group of green macroalgae, which are cosmopolitan
33 species, both ecologically and economically. Its highly adaptive nature allows it to flourish in various
34 environments, as can be seen from its widespread presence from the Arctic and Antarctic seas to the
35 Equator. In natural populations, *Ulva* spp. are very common in littoral and sublittoral areas and are also
36 sometimes found in mesophotic depths (Spalding et al., 2016; Pyle et al., 2016). As *Ulva* in nature is a
37 holobiome, its ecological role is vast and includes multiple interactions with other players of the marine
38 ecosystems, such as protista, fungi, bacteria, viruses and various marine fauna. *Ulva* is highly relevant for
39 aquaculture due to its fast growth rates and potential food, feed, materials, chemicals and energy
40 applications. Hence, *Ulva* is considered as a potential crop for controlled biomass production, onshore and
41 offshore (Fernand et al., 2017). Multiple reports in the last decade addressed *Ulva* aquaculture alone or in
42 multitrophic systems. In addition, *Ulva* biorefinery-enabling processes and technologies have made
43 immense progress in the production of starch, protein, cellulose, ulvan, salts, methane, biocrude, biodiesel,
44 bioethanol, and polyhydroxyalkanoates, just to mention a few (Bikker et al., 2016). Over the years, various
45 systems including plastic sleeves, raceway ponds, tanks, dripping, ropes, nets, rafts and aerated cages have
46 been proposed for *Ulva* biomass cultivation. The variation of cultivation systems ranges from closed,
47 artificial and seawater, onshore systems with fresh seawater to near shore and far offshore production. Yet,
48 one of the significant risks in *Ulva* cultivation is the sudden biomass loss when the algal tissue disintegrates
49 and bleaches, most probably caused by uncontrolled and unpredicted massive sporulation (Gao et al., 2010;
50 Bruhn et al., 2011).

51 Opposite to the controlled cultivation, *Ulva* green tides are massive, rapid natural accumulations of
52 unattached green macroalgae biomass usually associated with eutrophicated marine environments.
53 While green tides with *Ulva* species of folios morphology (distromatic sheets) prevail in many cases (Fort
54 et al., 2020; Zhao et al., 2019; Sfriso et al., 1992; Martins et al., 2001), there are also mass occurrences of
55 the monostromatic tubular form (Gao et al., 2010; Cai et al., 2021; Blomster et al., 2002), which is of
56 particular importance in our study. Nonetheless, the impact of thalli morphology on the potential of *Ulva*
57 species to generate green tides is yet to be determined.

58

59 Nevertheless, green tides seriously damage the coastal marine environment, on occasions modifying the
60 shoreline structure, or affecting biodiversity and damaging ecosystem services such as navigation, fishery
61 and recreation (Shan et al., 2019; Zhang et al., 2019). In addition, decaying seaweed biomass causes anoxia
62 yielding hydrogen sulfide at toxic levels in coastal waters and on the shores (Nedergaard et al., 2002; Castel
63 et al., 1996; Viaroli et al., 1995).

64
65 Various explanations have been proposed for the rapid accumulation and simultaneous collapse of *Ulva*
66 dominated green tides. Favorable environmental conditions for *Ulva* habitats, such as temperature, salinity,
67 hydrodynamics and nutrient levels affect the rapid biomass growth. In addition, recent studies showed that
68 blooming leads to the selection of rapidly growing strains (Fort et al., 2020) with potentially differentially
69 expressed genetic signatures (He et al., 2021). Furthermore, for *Ulva prolifera*, a strain dominating the
70 Yellow Sea bloom, 91.6–96.4 % of the released spores developed into young seedlings, suggesting that 1
71 gFW thallus was able to produce about 2.8×10^8 – 2.7×10^9 new younger seedlings, of free-floating biomass
72 (Zhang et al., 2013).

73
74 *Ulva* sp. has a complex reproduction strategy with alternation of generations in which both isomorphic
75 gametophytes and sporophytes coexist. The gametophytes produce biflagellated haploid gametes through
76 mitosis while the sporophytes produce quadriflagellated haploid zoids through meiosis (Wichard, 2015).
77 The initiation of a green tide requires simultaneous sporulation and release of gametes of multiple thalli
78 (Gao et al., 2010), but can be also caused by inhibition of biomass allocation to sporulation (Hiraoka, 2021).
79 In any case the regulation of sporulation is involved. How this sporulation is achieved and controlled at
80 the initial population is still a puzzling question. The simultaneous release of zoids and gametes in large
81 numbers over a short period, combined with favorable environmental conditions, would provide the
82 prerequisites for the formation of green tides. Indeed, mechanical or other factors, fragmentation of *Ulva*
83 thalli would produce large amounts of spores giving rise to the rapid proliferation of the seaweed under
84 field conditions. This idea was also considered since it likely supports the rapid accumulation of huge
85 biomass of *U. prolifera* in the green tide observed along the Qingdao coasts in 2008 (Gao et al., 2010).

86 Ecological studies indicate that sporulation in *Ulva* is seasonal, and when it occurs a significant amount of
87 parental biomass contributes to the massive production of swimmers (Amsler and Searles, 1980; Littler and
88 Littler, 1980; Niesenbaum, 1988). The formation and release of swimmers is inhibited by “sporulation-
89 inhibiting substances” excreted into the growth medium by the whole thalli, or their fragments (Nilsen and
90 Nordby, 1975; Jónsson et al., 1985). Later studies identified sporulation inhibitors in *Ulva mutabilis*, *Ulva*
91 *linza* and *U. prolifera*. The first sporulation inhibitor 1 (SI-1), is a glycoprotein isolated from the thalli
92 media or the cell wall and the second sporulation inhibitor 2 (SI-2), is a small molecular weight compound
93 that was isolated from the inner space between the two blade cell layers. (Stratmann et al., 1996; Jónsson
94 et al., 1985; Kessler et al., 2018; Vesty et al., 2015). Importantly, removing both SIs induces the
95 gametogenesis by washing (and mincing) the algae (Kessler et al., 2018) and activates specific transcription
96 factors (Liu et al., 2022).

97
98 Further **more, formed gametes** were only released slowly and asynchronously in the presence of another
99 substance known as a swarming inhibitor, the removal of which resulted in nearly immediate and complete
100 swarming (Stratmann et al., 1996; Wichard and Oertel, 2010). This precise control of swarmer formation
101 and release suggests that *Ulva* developed a tightly regulated mechanism to guarantee simultaneous release
102 of swarmer to the environment, observed initially by Smith (1947) at the Pacific coast (Smith, 1947),
103 probably to maximize the likelihood of sexual reproduction. Indeed, most recent studies on the floating
104 *Ulva prolifera* showed that all tested thalli were sporophytes with sexual reproductive patterns (Zhao et al.,
105 2019).

106
107 Notably, the decrease of SI-1 production coincides with the maturation of *Ulva* and finally causes
108 sporulations (i.e. gametogenesis), first within the *Ulva* apical marginal zones of the thallus and subsequently
109 within the whole alga. Unlike the SI-1, the concentration of SI-2 (per biomass) remains constant, but *Ulva's*
110 sensitivity towards this inhibitor declines during aging (Stratmann et al. 1996). Unlike SI-2, the presence
111 of SI-1 suppresses gametogenesis at all phases of the life cycle (Fig. 1). In other words, even if *Ulva* no
112 longer produces enough SI-1 during aging, it is still sensitive to external SI-1 application by an aquaculture
113 operator (Fig. 1).

114 Because only one of the two inhibitors is required to be present and active (Stratmann et al. 1996, Vesty et
115 al. 2015; Kessler et al. 2018), our research concentrates on mathematical model experiments with SI-1,
116 which is produced by the growing *Ulva*, released in excess in its environment and taken up by aging *Ulva*.

117



118

119 **Figure 1.** Inhibition of gametogenesis by an externally supplied sporulation inhibitor (SI-1). Two thalli (1 and 2) were
120 transferred into fresh UCM distributed over two Petri dishes. Mature gametophytes undergo gametogenesis upon
121 removal of SIs by washing the thalli. Within three days, gametes were formed and released on the third day after
122 induction (left). The addition of 10 units of SI-1 inhibited the differentiation of thallus cells into gametangia (right)
123 (see Supplementary Information for detailed method description according to Kessler et al. (2018)).

124
125 Mathematical models are essential tools to study and predict the behavior of complex biological systems.
126 Several models have been developed to predict seaweed biomass growth and decomposition, the behavior
127 of harmful green tides and the seaweed biomass production in seagrass culture. Indeed, long-term ecological
128 models that predict macroalgal productivity and seasonal blooms in prone ecosystems (Martins and
129 Marques, 2002; Solidoro et al., 1997; Ren et al., 2014; Martins et al., 2007; Port et al., 2015; Brush and
130 Nixon, 2010; Aldridge and Trimmer, 2009; Lavaud et al., 2020; Seip, 1980; Aveytua-Alcázar et al., 2008;
131 Duarte and Ferreira, 1997) or culture models that focus mostly on onshore photobioreactors (Friedlander et
132 al., 1990; Oca Baradad et al., 2019) and offshore cultivation (Broch and Slagstad, 2012; Petrell et al., 1993;
133 Hadley et al., 2015) were developed. These models, which pursue a basic understanding of the
134 thermodynamics of individual algae thalli and photobioreactors (Zollmann et al., 2018; Lehahn et al., 2016;
135 Martins and Marques, 2002; Lee and Ang Jr, 1991; Seip, 1980), provide important tools to predict the
136 productivity and seasonal environmental effects on the seaweed population dynamics. However, such
137 models treat the macroalgae population as a bulk and do not differentiate between ages of individual thalli
138 within the population. As discussed above, thalli age is an important factor affecting the activity of
139 sporulation inhibitors in the alga and the ultimate release of swimmers. Furthermore, these models do not
140 consider the possible interthalli chemical interactions, some of which can be based on SI-1 secreted to the
141 environment. The production and secretion to the environment of molecules such as SI-1 could provide
142 insights into the molecular mechanisms behind the synchronization of massive spore release at the
143 population level - a phenomenon crucial for both green tide formation and sudden biomass disappearance
144 in *Ulva* seagrass culture of species such as *U. mutabilis* (*U. compressa*), *U. linza* and *U. prolifera*.

145 This paper aims to introduce a novel framework for the description of population dynamics and collective
146 thalli behavior of *Ulva* biomass, presumably controlled by shared sporulation inhibitors. We propose that
147 various environmental and internal biological changes on the single thallus level predetermine the ability
148 of the individual thallus to produce, and to donate to and receive from the population environment, factors
149 that regulate the synchronized formation and release of swimmers. A natural tool to describe this process is
150 offered by population dynamics models, often employed to describe bacterial and animal population
151 dynamics (Succurro and Ebenhöf, 2018; Friedman and Gore, 2017).

152 In the following sections we develop and simulate such a mathematical model in an attempt to characterize
 153 the dynamics of *Ulva* biomass formation and degradation.

154 2. Methods

155 The model presented below consists of $n+1$ ordinary differential equations (ODEs), where n is set as the
 156 number of cultivation days (also equal to the number of age group equations). ODEs $0 \dots n-1$ describe the
 157 rate of change of biomass of n discrete age classes of *Ulva* thalli, denoted a_i , and an additional $n+1$ equation
 158 for the rate of change of the inhibitor I . As described previously, there are at least three types of inhibitors
 159 involved in the process of *Ulva* swimmers release: SI-1, SI-2 and a swarming inhibitor (SWI). We aggregate
 160 these inhibitors into a single quantity that controls the simultaneous swimmers' release from thalli, followed
 161 by the biomass decrease.

162 The n ODEs follow a simple discretized version of a partial differential equation of $m(a,t)$ where m is the
 163 biomass of *Ulva* in controlled volume (a bioreactor or a given sea volume, for example), a is the age of
 164 algae, and t is time. As previously shown, the growth rate for thalli decreases with age in *U. mutabilis*
 165 (Alsufyani et al., 2017).

166 The following equations specify the dynamics of the biomass of each age class a_i , coupled with the
 167 dynamics of the inhibitor I , in the growth environment:

$$168 \frac{da_i}{dt} = r_i \left(1 - \frac{\sum_i^a a_i}{K}\right) + \lambda_i a_{i-1} - \lambda_{i+1} a_i - \sigma a_i f(I) \quad i = 1, 2 \dots n \quad (1)$$

$$169 \frac{dI}{dt} = \sum_i^n a_i \theta_i - I(\sum_i^n \mu_i a_i) - \xi I + \gamma_I \quad (2)$$

170

171 **Table 1:** model parameters, their interpretation, and values.

Parameter	Meaning	Value
r_i	Growth rate of algae age a_i	$0.45 \left(0.1 + e^{-i \frac{\log(2)}{30}}\right)$
$f(I)$	Limiting factor due to inhibitor concentration, I	$1 - \left(1 + e^{-10(I-0.5)}\right)^{-1}$
σ	Degradation constant	0.3
ξ	Inhibitor loss function to the environment (for example, water replacement)	$0.45 \left(0.1 + e^{-i \frac{\log(2)}{120}}\right)$

θ_i	Age-dependent inhibitor generation function	$0.45 \left(0.1 + e^{-i \frac{\log(2)}{120}} \right)$
μ_i	Age-dependent inhibitor uptake	$0.45 \left(0.05 + e^{-i \frac{\log(2)}{120}} \right)$
γ_I	Constant inhibitor addition or extraction	0.0 - 0.1 (varies in the figures)
K	Maximal carrying capacity	10 kg m ⁻³
a_{in}	Initial density	0.2 kg m ⁻³

172

173 The model assumes a logistic growth of biomass with a growth rate parameter r_i for each algae age class
174 a_i and a carrying capacity K , defined as the maximum *Ulva* biomass density in the growth environment.
175 Biomass moves between compartment a_i to a_{i+1} at rates λ_i , defining the “natural aging” of algae. At each
176 age class a_i , biomass is degraded at a rate $\sigma f(I)$, where σ is the maximal destruction rate, and $f(I)$ is a
177 monotonically decreasing function of the inhibitor I (SI-1), scaled between zero and one. The degradation
178 at a rate $\sigma = 0.3$ is a conservative approximation estimated from a closed aquaculture system with *U.*
179 *mutabilis* (Alsufyani et al., 2020).

180 Furthermore, we define μ_i as the SI-1 uptake rate of each age class a_i ; ξ the leakage or injection of the
181 inhibitor I , that can be managed externally to the system (e.g., washing the algae, destroying the algae,
182 injection nutrients); and γ is the nutrient supply flux in the units of inhibitor concentration. Since this is a
183 novel theoretical model, there were no available empirical estimates of the specific functions underlying
184 its dynamics. Hence, whenever a rate was modeled as some monotonic function which saturates, we used
185 the standard in ecological modeling - the logistic equation and exponential decay (Jørgensen and
186 Bendoricchio, 2001). The model functions and parameters are summarized in Table 1.

187 Finally, we note that our model does not take into account addition of new thalli due to sporulation events
188 during the simulated timeframe. This may be construed as simulating an experiment where spores freely
189 flow out of the container used for growing the algae (e.g., (Prabhu et al., 2020)). Or, this may serve as an
190 approximation if the amount of new thalli produced by sporulation in the simulated experimental time frame
191 can be neglected.

192

193 3. Results and Discussion

194 Here, we study the *Ulva* biomass population dynamics, controlled by sporulation inhibitor production and
195 absorption, by simulating the biomass accumulation under various scenarios for mixed-age populations, for

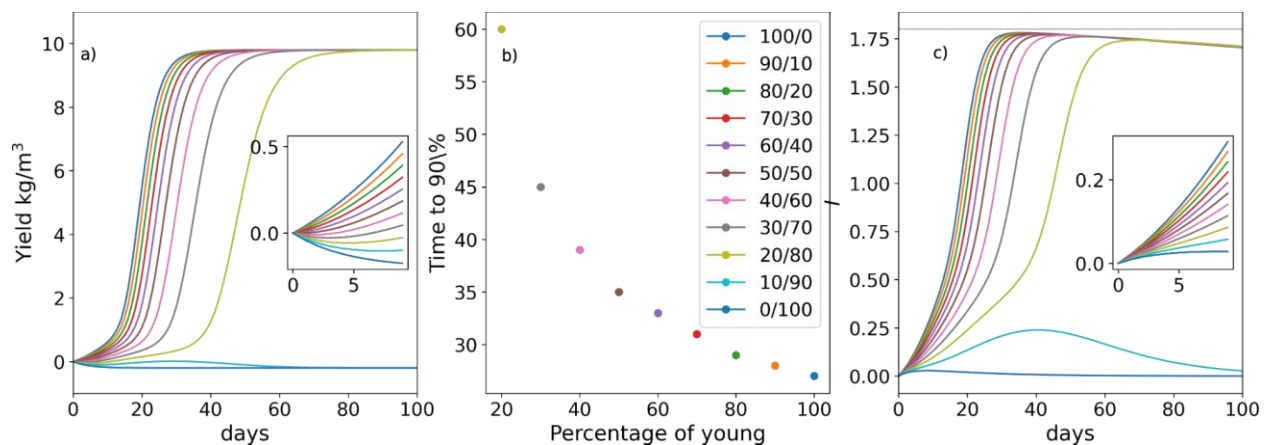
196 100 days (Stratmann et al., 1996; Alsufyani et al., 2017). In all the following simulations, we set the initial
197 density of seaweed in the cultivation media to $a_{in} = 0.2 \text{ kg m}^{-3}$, and at the maximum carrying capacity the
198 biomass can reach a density of 10 kg m^{-3} (K). In addition, for the initial population conditions, we denoted
199 young thalli as the population of a_0 at $t = 0$ and old thalli as the population of a_{120} at $t = 0$. From a
200 physiological point of view, young thalli are those thalli, whose cell differentiation is controlled by SI and
201 old thalli are those thalli, which are insensitive to SI and do not produce it.

202
203 In the following plots, we simulated the behavior of populations with a mixed-age composition. Each
204 population was labeled by the percentage of young and old thalli at initial population. Thus, for example,
205 100/0 labels an entirely young initial population (0.2 kg m^{-3} of thalli with $a_i = 0$ at $t = 0$); 0/100 labels a
206 completely old initial population (0.2 kg m^{-3} of thalli with $a_i = 120$ days at $t = 0$); and 50/50 represents an
207 initial population comprised of equal parts of old and young algae (0.1 kg m^{-3} of thalli with $a_i = 0$ at $t = 0$
208 and 0.1 kg m^{-3} of thalli with $a_i = 120$ days at $t = 0$).

209
210 The biomass yield (density increase due to growth; i.e. initial density subtracted from final density) over
211 time for various mixed-age populations is shown in **Fig. 2a**. The growth of mixed aged populations with
212 100/0, 80/20 and 50/50 population mix of old and young thalli showed a typical sigmoidal growth, reaching
213 90% of the maximum biomass density (9 kg m^{-3}) at 27, 30 and 37 days, respectively. Populations with
214 predominantly old biomass at the beginning (20/80) showed a long lag phase but exhibited positive growth,
215 reaching 90% of the maximum biomass density at day 87 (**Fig. 2b**). The population with only old algae
216 (0/100) at the beginning of the cultivation showed degradation of the biomass from day 1 and never showed
217 positive growth (**Fig. 2b**). The population with a 10/90 mix of initial ages showed a small growth (positive
218 yield) during the first 40 days but then showed biomass degradation and never reached 90% of the
219 maximum density (**Fig. 2a,b**).

220
221 As simulated in our model, such dynamics of the biomass growth could be explained by the dynamics of
222 the production of the sporulation inhibitor (**Fig. 2c**). For populations 100/0, 80/20, 50/50 and 20/80 the rate
223 of sporulation inhibitor generation is positive and increases over time, while for the 10/90 and 0/100
224 populations, although initial production of the sporulation inhibitor is observed, it is reduced over time (**Fig.**
225 **2c**). These findings show that sporulation inhibitor production by a small (20% in our simulations) young
226 population could potentially provide enough inhibitor to prevent the old algae population from biomass
227 loss, thus leading to overall positive biomass production. Additionally, the rate of biomass accumulation
228 increases with the increased fraction of the young thalli in the initial population. Nevertheless, the maximum
229 inhibitor production decreases with time in all populations as all thalli age (**Fig. 2c**). To account for a less

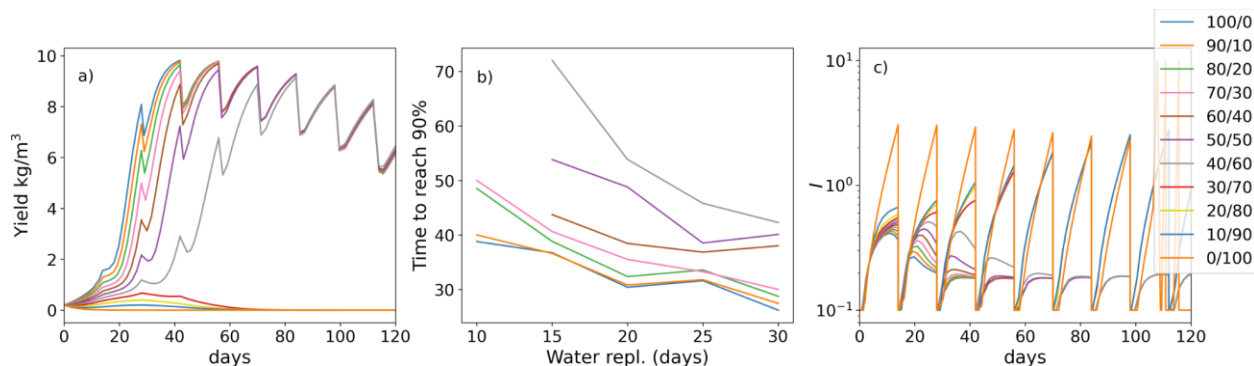
230 homogeneous initial population structure, the dynamics were also simulated with a different initial
 231 distributions of ages, and produced qualitatively similar results (Supplemental Information Figure S1).
 232



233
 234 **Figure 2. a.** Yield for populations with various initial age mixes (biomass gain in kg/m^3 up to the limit of $10 \text{ kg}/\text{m}^3$
 235 in a bioreactor with a starting density of $0.2 \text{ kg}/\text{m}^3$ in total for each simulated age mix [old / young thalli in %]). **b.**
 236 *Ulva* biomass growth kinetics as a function of the initial age distribution of thalli in the population. Values of the
 237 0/100, and 10/90 populations are not presented as they did not reach 90% of the maximal carrying capacity. In any
 238 other case, mixed populations achieved at least 90% of the maximal biomass carrying capacity **c.** Inhibitor amount in
 239 the system over time. Insets in (a) and (c) present zoomed-in dynamics during the first 10 days.

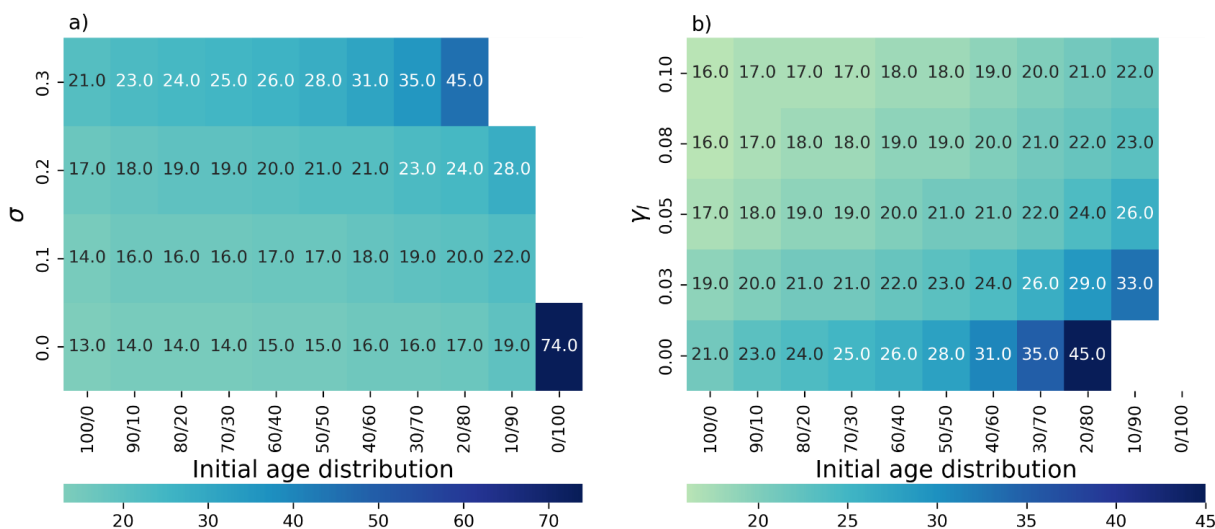
240 As seaweeds rarely grow in closed bodies of water, where the inhibitor could accumulate continuously in
 241 the environment, we sought to stimulate the impact of inhibitor removal from the seaweed environment by
 242 water replacement. We simulate each event of water replacement as complete removal of the inhibitor
 243 produced by the seaweed during the time interval from the previous water replacement. **Figure 3a** shows
 244 the dynamics of various initial age mixed populations yields when the inhibitor is removed by water
 245 replacement. In the scenario where water is replaced every 14 days, only few, relatively “young”
 246 populations (100/0, 90/10, 80/20 and 70/30) achieved the 90% of the maximum yield. Moreover, the time
 247 to reach this yield level increased from 27-30 days (without replacement for these four age groups) to 37-
 248 40 days, in the 100/0, 90/10, 80/20 and 70/30 populations, respectively (**Fig. 3b**). The growth yield shows
 249 fluctuating dynamics, showing in the initial overall growth for populations with predominantly young thalli
 250 during the first 60 cultivation days, followed by the overall reduction of the yield in the aging populations.
 251 Interestingly, these fluctuations yield dynamics that are similar to those previously reported by us during a
 252 12-month offshore cultivation work with *Ulva* harvesting every week (Chemodanov et al., 2018). Although
 253 many other factors could be at play, it is possible that the weekly removal of the whole seaweed biomass
 254 from the sea and cages for weighting also removed the sporulation inhibitor accumulated in the boundary

255 layer near the thalli. This suggestion, of course, requires further detailed experiments investigating the
 256 ability to monitor the dynamics of sporulation inhibitors production and accumulation/diffusion in the thalli
 257 environment. In our simulations, increasing the frequency of water exchange, and thus removal of SI-1
 258 (**Fig. 3c**), reduced the ability of populations with a large portion of old algae to produce a positive yield
 259 during the whole cultivation period (**Fig. 3a**).



260
 261
 262 **Figure 3. a.** Yield (biomass gain in kg/m³ up to the limit of 10 kg/m³ in a bioreactor with a starting density of 0.2
 263 g/m³) for populations with various initial age mixes [% of old / young thalli] with 14 days water replacement
 264 frequency. **b.** *Ulva* biomass growth kinetics as a function of the initial age distribution of thalli in the population with
 265 various frequencies of water replacement. **c.** Inhibitor production in the population of the time with 14 days of water
 266 replacement frequency.

267 As seaweed in the natural environment usually live in high energy conditions, we also studied the coupled
 268 effects of degradation (σ) and population age distribution on the ability of the population biomass yield
 269 (**Fig. 4a**). Higher rates of degradation prevent positive yields in all mixed-age populations. Lower
 270 degradation affects a smaller portion of the population with higher initial portions of young thalli (**Fig. 4a**)
 271 showing again the regenerative ability of the populations with high growth (lower sporulation) capabilities.



272
 273 **Figure 4.** a. Time to achieve 90% of the maximum carrying capacity as a heatmap (color represents the time in days)
 274 depending on the initial age distribution (x-axis; [% of old / young thalli]) and the degradation parameter σ_i (y-axis).
 275 b. Time to 90% as a heatmap (color represents the time in days; note the different scales in (a) and (b)) depending on
 276 the initial age distribution (x-axis) and the addition of the external inhibitor γ (y-axis). White color means that the
 277 population never achieves 90% of the maximum carrying capacity.

278
 279 We investigated the impact of direct addition of the sporulation inhibitor to the seaweed growth media
 280 computationally. Adding an external sporulation inhibitor (up to 0.1) reduced the time to achieve 90% of
 281 the maximum yield from 27 days (without inhibitor addition) to 21 days for 100/0 group, 29 days (without
 282 inhibitor addition) to 24 for 80/20 group, from 35 days (without inhibitor addition) to 28 for the 50/50 group
 283 and from 60 (without inhibitor addition) to 45 days for the 20/80 group. No effects at this maximum
 284 concentration have been observed for the 0/100 group.

285 4. Conclusions

286 In this study, we aimed to further understand the growth and sporulation dynamics of *Ulva* using a
 287 mathematical model. We found that successful accumulation of *Ulva* biomass depends on the age
 288 distribution of the *Ulva* thalli of a given seedstock, where older starter populations produce lower yields at
 289 a given time. However, this age-dependent effect can be mitigated, leading to prolonged maintenance of
 290 *Ulva*'s aquacultures, by external addition of sporulation inhibitors. We note that our modeling study is a
 291 first attempt to uncover the mechanism underlying the heterogeneity of vegetative growth stability in
 292 different *Ulva* populations. At this point, we developed a general model, which is not species specific.

293 Indeed, several studies have revealed that the SIs of *U. linza*, *U. compressa* (*U. mutabilis*), and *U.*
294 *intestinalis* are exchangeable (Vesty et al., 2015; Steinhagen et al., 2019; Stratmann et al., 1996). We
295 assume the more closely related the *Ulva* species are, the more likely the SIs will be interchangeable
296 between the species. The SI-1, in fact, cannot be swapped between *U. compressa* and *U. rigida* (Stratmann
297 et al., 1996).

298 Bioassays with SI-1 have backed up the finding of the model that age-mixed populations are more stable
299 than uniform ones. When purified SI-1 is added to mature and induced *Ulva* thalli, it can be perceived by
300 *Ulva* and used to regulate gametogenesis of cultures of the 100/0 group. We thus conclude that the
301 sporulation event is delayed or even inhibited in age-mixed cultures composed of young, smaller thalli and
302 old, larger thalli.

303 Overall the sporulation phenomenon creates unique constraints on the age structure of *Ulva* populations.
304 In higher plants, sexual reproduction and vegetative propagation compete for nutrients, but the competition
305 may be mitigated by separating these processes through time (Evans and Black, 1993). However, in *Ulva*,
306 the whole thallus can be transformed into gametangia and sporangia while flowering plants assign only a
307 specific portion of biomass to reproductive structures. *Ulva* thus requires a strict regulation of sporulation,
308 e.g. through the age-dependent production of SI. Only if the SI-1 synthesis ceases during the *Ulva*'s
309 development cycle and its concentration falls below a critical threshold concentration, gametogenesis is
310 induced at positions of the blade where the SI-2 concentration between the cell layers is also sufficiently
311 low or not perceived anymore (Stratmann et al., 1996). Our findings thus imply that the more SI provided
312 by young algae in mixed cultures, the higher the growth rate and biomass yields. As purified SIs are not yet
313 widely available in large quantities, the use of mixed-aged cultures can be an important tool to maintain
314 them at adequate nutrient levels e.g. in integrated multi trophic aquaculture. The modeling of *Ulva*'s growth
315 indicates the importance of SI-producing algae for sustainable and successful seagrass, and paves the
316 way for a better understanding of the green tide formation in coastal areas.

317

318 **5. Code availability**

319 The model creation process is explained in detail in the Methods. Code for creating the figures is available
320 upon request.

321 **6. Author contributions**

322 AG and AL conceived the initial idea for the study; UO, AG and AL designed the study and the
323 mathematical model; AL produced the results; TW produced the experimental results; All authors
324 interpreted the results and wrote the manuscript.

325 **7. Acknowledgements**

326 Ralf Kessler (Friedrich Schiller University Jena, Germany) is acknowledged for carrying out the shown
327 biotest with *Ulva*. The authors thank the Israel Ministry of Health (grant #3-16052) for the support. This
328 article is based upon work from COST Action CA20106, supported by COST (European Cooperation in
329 Science and Technology, www.cost.eu).

330 **8. Competing interests**

331 The authors declare that they have no conflict of interest.

332

333

334

335

336 References

- 337 Aldridge, J. and Trimmer, M.: Modelling the distribution and growth of ‘problem’ green seaweed in the
338 Medway estuary, UK, in: *Eutrophication in Coastal Ecosystems*, Springer, 107–122, 2009.
- 339 Alsufyani, T., Weiss, A., and Wichard, T.: Time course exo-metabolomic profiling in the green marine
340 macroalga *Ulva* (Chlorophyta) for identification of growth phase-dependent biomarkers, *Mar. Drugs*, 15,
341 14, 2017.
- 342 Alsufyani, T., Califano, G., Deicke, M., Grueneberg, J., Weiss, A., Engelen, A. H., Kwantes, M., Mohr, J.
343 F., Ulrich, J. F., and Wichard, T.: Macroalgal–bacterial interactions: identification and role of thallusin in
344 morphogenesis of the seaweed *Ulva* (Chlorophyta), *J. Exp. Bot.*, 71, 3340–3349, 2020.
- 345 Amsler, C. D. and Searles, R. B.: VERTICAL DISTRIBUTION OF SEAWEED SPORES IN A WATER
346 COLUMN OFFSHORE OF NORTH CAROLINA 1, *J. Phycol.*, 16, 617–619, 1980.
- 347 Aveytua-Alcázar, L., Camacho-Ibar, V. F., Souza, A. J., Allen, J., and Torres, R.: Modelling *Zostera*
348 *marina* and *Ulva* spp. in a coastal lagoon, *Ecol. Model.*, 218, 354–366, 2008.
- 349 Bikker, P., van Krimpen, M. M., van Wikselaar, P., Houweling-Tan, B., Scaccia, N., van Hal, J. W.,
350 Huijgen, W. J., Cone, J. W., and López-Contreras, A. M.: Biorefinery of the green seaweed *Ulva lactuca*
351 to produce animal feed, chemicals and biofuels, *J. Appl. Phycol.*, 28, 3511–3525, 2016.
- 352 Blomster, J., Bäck, S., Fewer, D. P., Kiirikki, M., Lehvo, A., Maggs, C. A., and Stanhope, M. J.: Novel
353 morphology in *Enteromorpha* (Ulvophyceae) forming green tides, *Am. J. Bot.*, 89, 1756–1763, 2002.
- 354 Broch, O. J. and Slagstad, D.: Modelling seasonal growth and composition of the kelp *Saccharina*
355 *latissima*, *J. Appl. Phycol.*, 24, 759–776, 2012.
- 356 Bruhn, A., Dahl, J., Nielsen, H. B., Nikolaisen, L., Rasmussen, M. B., Markager, S., Olesen, B., Arias, C.,
357 and Jensen, P. D.: Bioenergy potential of *Ulva lactuca*: biomass yield, methane production and
358 combustion, *Bioresour. Technol.*, 102, 2595–2604, 2011.
- 359 Brush, M. J. and Nixon, S. W.: Modeling the role of macroalgae in a shallow sub-estuary of Narragansett
360 Bay, RI (USA), *Ecol. Model.*, 221, 1065–1079, 2010.
- 361 Cai, C., Gu, K., Zhao, H., Steinhagen, S., He, P., and Wichard, T.: Screening and verification of
362 extranuclear genetic markers in green tide algae from the Yellow Sea, *PloS One*, 16, e0250968, 2021.
- 363 Castel, J., Caumette, P., and Herbert, R.: Eutrophication gradients in coastal lagoons as exemplified by
364 the Bassin d’Arcachon and the Etang du Prévost, *Hydrobiologia*, 329, ix–xxviii, 1996.
- 365 Chemodanov, A., Jinjikhashvily, G., Habiby, O., Liberzon, A., Israel, A., Yakhini, Z., and Golberg, A.:
366 Net primary productivity, biofuel production and CO₂ emissions reduction potential of *Ulva*
367 sp.(Chlorophyta) biomass in a coastal cPdatcc area of the Eastern Mediterranean (vol 148, pg 1497,
368 2017), *Energy Convers. Manag.*, 166, 772–772, 2018.
- 369 Duarte, P. and Ferreira, J.: A model for the simulation of macroalgal population dynamics and
370 productivity, *Ecol. Model.*, 98, 199–214, 1997.
- 371 Evans, R. and Black, R. A.: Growth, photosynthesis, and resource investment for vegetative and
372 reproductive modules of *Artemisia tridentata*, *Ecology*, 74, 1516–1528, 1993.

373 Fernand, F., Israel, A., Skjermo, J., Wichard, T., Timmermans, K. R., and Golberg, A.: Offshore
374 macroalgae biomass for bioenergy production: Environmental aspects, technological achievements and
375 challenges, *Renew. Sustain. Energy Rev.*, 75, 35–45, 2017.

376 Fort, A., Mannion, C., Fariñas-Franco, J. M., and Sulpice, R.: Green tides select for fast expanding *Ulva*
377 strains, *Sci. Total Environ.*, 698, 134337, 2020.

378 Friedlander, M., Galai, N., and Farbstein, H.: A model of seaweed growth in an outdoor culture in Israel,
379 *Hydrobiologia*, 204, 367–373, 1990.

380 Friedman, J. and Gore, J.: Ecological systems biology: The dynamics of interacting populations, *Curr.*
381 *Opin. Syst. Biol.*, 1, 114–121, 2017.

382 Gao, S., Chen, X., Yi, Q., Wang, G., Pan, G., Lin, A., and Peng, G.: A strategy for the proliferation of
383 *Ulva prolifera*, main causative species of green tides, with formation of sporangia by fragmentation, *PLoS*
384 *One*, 5, e8571, 2010.

385 Hadley, S., Wild-Allen, K., Johnson, C., and Macleod, C.: Modeling macroalgae growth and nutrient
386 dynamics for integrated multi-trophic aquaculture, *J. Appl. Phycol.*, 27, 901–916, 2015.

387 He, Y., Shen, S., Yu, D., Wang, Y., Yin, J., Wang, Z., and Ye, Y.: The *Ulva prolifera* genome reveals the
388 mechanism of green tides, *J. Oceanol. Limnol.*, 1–13, 2021.

389 Hiraoka, M.: Massive *Ulva* Green Tides Caused by Inhibition of Biomass Allocation to Sporulation,
390 *Plants*, 10, 2482, 2021.

391 Jónsson, S., Laur, M.-H., and Pham-Quang, L.: Mise en évidence de différents types de glycoprotéines
392 dans un extrait inhibiteur de la gamétogénèse chez *Enteromorpha prolifera*, *Chlorophycée marine*,
393 *Cryptogam. Algol.*, 6, 253–264, 1985.

394 Jørgensen, S. E. and Bendoricchio, G.: *Fundamentals of ecological modelling*, Elsevier, 2001.

395 Kessler, R. W., Alsufyani, T., and Wichard, T.: Purification of sporulation and swarming inhibitors from
396 *Ulva*, *Protoc. Macroalgae Res.*, 139–58, 2018.

397 Lavaud, R., Filgueira, R., Nadeau, A., Steeves, L., and Guyondet, T.: A Dynamic Energy Budget model
398 for the macroalga *Ulva lactuca*, *Ecol. Model.*, 418, 108922, 2020.

399 Lee, C. and Ang Jr, P.: A simple model for seaweed growth and optimal harvesting strategy, *Ecol.*
400 *Model.*, 55, 67–74, 1991.

401 Lehahn, Y., Ingle, K. N., and Golberg, A.: Global potential of offshore and shallow waters macroalgal
402 biorefineries to provide for food, chemicals and energy: feasibility and sustainability, *Algal Res.*, 17,
403 150–160, 2016.

404 Littler, M. M. and Littler, D. S.: The evolution of thallus form and survival strategies in benthic marine
405 macroalgae: field and laboratory tests of a functional form model, *Am. Nat.*, 116, 25–44, 1980.

406 Liu, X., Blomme, J., Bogaert, K., D’hondt, S., Wichard, T., Thomas, Deforce, D., Van Nieuwerburgh, F.,
407 and De Clerck, O.: Transcriptional profiling of gametogenesis in the green seaweed *Ulva mutabilis*
408 identifies an RWP-RK transcription factors linked to reproduction, *BMC Plant Biol.*, 22, 19, 2022.

409 Martins, I. and Marques, J.: A model for the growth of opportunistic macroalgae (*Enteromorpha* sp.) in
410 tidal estuaries, *Estuar. Coast. Shelf Sci.*, 55, 247–257, 2002.

- 411 Martins, I., Pardal, M., Lillebø, A., Flindt, M., and Marques, J.: Hydrodynamics as a major factor
412 controlling the occurrence of green macroalgal blooms in a eutrophic estuary: a case study on the
413 influence of precipitation and river management, *Estuar. Coast. Shelf Sci.*, 52, 165–177, 2001.
- 414 Martins, I., Lopes, R., Lillebø, A., Neto, J., Pardal, M., Ferreira, J., and Marques, J.: Significant variations
415 in the productivity of green macroalgae in a mesotidal estuary: implications to the nutrient loading of the
416 system and the adjacent coastal area, *Mar. Pollut. Bull.*, 54, 678–690, 2007.
- 417 Nedergaard, R. I., Risgaard-Petersen, N., and Finster, K.: The importance of sulfate reduction associated
418 with *Ulva lactuca* thalli during decomposition: a mesocosm experiment, *J. Exp. Mar. Biol. Ecol.*, 275, 15–
419 29, 2002.
- 420 Niesenbaum, R. A.: The ecology of sporulation by the macroalga *Ulva lactuca* L.(Chlorophyceae), *Aquat.*
421 *Bot.*, 32, 155–166, 1988.
- 422 Nilsen, G. and Nordby, Ø.: A sporulation-inhibiting substance from vegetative thalli of the green alga
423 *Ulva mutabilis*, Føyn, *Planta*, 125, 127–139, 1975.
- 424 Oca Baradad, J., Cremades Ugarte, J., Jiménez de Ridder, P., Pintado, J., and Masaló Llorà, I.: Culture of
425 the seaweed *ulva ohnoi* integrated in a *Solea senegalensis* recirculating system, *J. Appl. Phycol.*, 31, 1–7,
426 2019.
- 427 Petrell, R., Tabrizi, K. M., Harrison, P., and Druehl, L.: Mathematical model of *Laminaria* production
428 near a British Columbian salmon sea cage farm, *J. Appl. Phycol.*, 5, 1–14, 1993.
- 429 Port, A., Bryan, K. R., Pilditch, C. A., Hamilton, D. P., and Bischof, K.: Algebraic equilibrium solution of
430 tissue nitrogen quota in algae and the discrepancy between calibrated parameters and physiological
431 properties, *Ecol. Model.*, 312, 281–291, 2015.
- 432 Prabhu, M., Levkov, K., Levin, O., Vitkin, E., Israel, A., Chemodanov, A., and Golberg, A.: Energy
433 efficient dewatering of far offshore grown green macroalgae *Ulva* sp. biomass with pulsed electric fields
434 and mechanical press, *Bioresour. Technol.*, 295, 122229, 2020.
- 435 Pyle, R. L., Boland, R., Bolick, H., Bowen, B. W., Bradley, C. J., Kane, C., Kosaki, R. K., Langston, R.,
436 Longenecker, K., Montgomery, A., and others: A comprehensive investigation of mesophotic coral
437 ecosystems in the Hawaiian Archipelago, *PeerJ*, 4, e2475, 2016.
- 438 Ren, J. S., Barr, N. G., Scheuer, K., Schiel, D. R., and Zeldis, J.: A dynamic growth model of macroalgae:
439 application in an estuary recovering from treated wastewater and earthquake-driven eutrophication,
440 *Estuar. Coast. Shelf Sci.*, 148, 59–69, 2014.
- 441 Seip, K. L.: A computational model for growth and harvesting of the marine alga *Ascophyllum nodosum*,
442 *Ecol. Model.*, 8, 189–199, 1980.
- 443 Sfriso, A., Pavoni, B., Marcomini, A., and Orio, A.: Macroalgae, nutrient cycles, and pollutants in the
444 Lagoon of Venice, *Estuaries*, 15, 517–528, 1992.
- 445 Shan, J., Li, J., and Xu, Z.: Estimating ecological damage caused by green tides in the Yellow Sea: A
446 choice experiment approach incorporating extended theory of planned behavior, *Ocean Coast. Manag.*,
447 181, 104901, 2019.
- 448 Smith, G. M.: On the reproduction of some Pacific coast species of *Ulva*, *Am. J. Bot.*, 80–87, 1947.
- 449 Solidoro, C., Pecenik, G., Pastres, R., Franco, D., and Dejak, C.: Modelling macroalgae (*Ulva rigida*) in

450 the Venice lagoon: Model structure identification and first parameters estimation, *Ecol. Model.*, 94, 191–
451 206, 1997.

452 Spalding, H. L., Conklin, K. Y., Smith, C. M., O’Kelly, C. J., and Sherwood, A. R.: New Ulvaceae
453 (Ulvophyceae, Chlorophyta) from mesophotic ecosystems across the Hawaiian archipelago, *J. Phycol.*,
454 52, 40–53, 2016.

455 Steinhagen, S., Barco, A., Wichard, T., and Weinberger, F.: Conspecificity of the model organism *Ulva*
456 *mutabilis* and *Ulva compressa* (Ulvophyceae, Chlorophyta), *J. Phycol.*, 55, 25–36, 2019.

457 Stratmann, J., Paputsoglu, G., and Oertel, W.: DIFFERENTIATION OF *ULVA MUTABILIS*
458 (CHLOROPHYTA) GAMETANGIA AND GAMETE RELEASE ARE CONTROLLED BY
459 EXTRACELLULAR INHIBITORS 1, *J. Phycol.*, 32, 1009–1021, 1996.

460 Succurro, A. and Ebenhöf, O.: Review and perspective on mathematical modeling of microbial
461 ecosystems, *Biochem. Soc. Trans.*, 46, 403–412, 2018.

462 Vesty, E. F., Kessler, R. W., Wichard, T., and Coates, J. C.: Regulation of gametogenesis and
463 zoosporogenesis in *Ulva linza* (Chlorophyta): comparison with *Ulva mutabilis* and potential for
464 laboratory culture, *Front. Plant Sci.*, 6, 15, 2015.

465 Viaroli, P., Bartoli, M., Bondavalli, C., and Naldi, M.: Oxygen fluxes and dystrophy in a coastal lagoon
466 colonized by *Ulva rigida* (Sacca di Goro, Po River Delta, northern Italy), *Fresenius Environ. Bull.*, 4, 381–
467 386, 1995.

468 Wichard, T.: Exploring bacteria-induced growth and morphogenesis in the green macroalga order Ulvales
469 (Chlorophyta), *Front. Plant Sci.*, 6, 86, 2015.

470 Wichard, T. and Oertel, W.: Gametogenesis and gamete release of *Ulva mutabilis* and *Ulva lactuca*
471 (Chlorophyta): regulatory effects and chemical characterization of the “swarming inhibitor” 1, *J. Phycol.*,
472 46, 248–259, 2010.

473 Zhang, J., Huo, Y., Yu, K., Chen, Q., He, Q., Han, W., Chen, L., Cao, J., Shi, D., and He, P.: Growth
474 characteristics and reproductive capability of green tide algae in Rudong coast, China, *J. Appl. Phycol.*,
475 25, 795–803, 2013.

476 Zhang, Y., He, P., Li, H., Li, G., Liu, J., Jiao, F., Zhang, J., Huo, Y., Shi, X., Su, R., and others: *Ulva*
477 *prolifera* green-tide outbreaks and their environmental impact in the Yellow Sea, China, *Natl. Sci. Rev.*,
478 2019.

479 Zhao, X., Cui, J., Zhang, J., Shi, J., Kang, X., Liu, J., Wen, Q., and He, P.: Reproductive strategy of the
480 floating alga *Ulva prolifera* in blooms in the Yellow Sea based on a combination of zoid and chromosome
481 analysis, *Mar. Pollut. Bull.*, 146, 584–590, 2019.

482 Zollmann, M., Traugott, H., Chemodanov, A., Liberzon, A., and Golberg, A.: Exergy efficiency of solar
483 energy conversion to biomass of green macroalgae *Ulva* (Chlorophyta) in the photobioreactor, *Energy*
484 *Convers. Manag.*, 167, 125–133, 2018.

485

486